



## 2D/3D hybrid structural model of vocal folds

Douglas Cook\*, Pradeep George, Margaret Julias

Division of Engineering, New York University, Abu Dhabi, UAE

### ARTICLE INFO

#### Article history:

Accepted 22 October 2011

#### Keywords:

Vocal fold  
Plane strain  
Phonation

### ABSTRACT

The spatial dimensionality of the vocal fold vibration is a common challenge in creating parsimonious models of vocal fold vibration. The ideal model is one that is accurate, with the lowest possible computational expense. Inclusion of full 3D flow and structural vibration typically requires massive amounts of computation, whereas reduction of either the flow or the structure to two dimensions eliminates certain aspects of physical reality, thus making the resulting models less accurate. Previous 2D models of the vocal fold structure have utilized a plane strain formulation, which is shown to be an erroneous modeling approach since it ignores influential stress components. We herein present a 2D/3D hybrid vocal fold model that preserves three-dimensional effects of length and longitudinal shear stresses, while taking advantage of a two-dimensional computational domain. The resulting model exhibits static and dynamic responses comparable to a 3D model, and retains the computational advantage of a two-dimensional model.

© 2011 Elsevier Ltd. All rights reserved.

### 1. Introduction

The modeling of human phonation presents a formidable challenge since this system involves complex fluid dynamics, structural vibration, acoustic propagation, and active control of the vocal apparatus. Modeling in any of these individual areas is not trivial, and the simultaneous coupling of all aspects compounds the difficulty of this task. Models of phonation by necessity thus rely upon simplifying assumptions. One of the most commonly applied assumptions is a reduction in the spatial dimensionality of the system: the fluid and solid domains have both been approximated as two-dimensional (Thomson et al., 2005; Decker and Thomson, 2007; Luo et al., 2008; Zhang, 2009), and the acoustic system is commonly approximated as one dimensional (Liljencrants, 1985; Story, 1995). While dimensionality assumptions provide reduced computational expense, they also introduce discrepancies between the model and reality. The discrepancies between 2D and 3D structural vocal fold models are the focus of this paper.

A review of the literature on vocal fold structural modeling revealed that the dimensionality of the vocal fold structure is not a new problem. In a series of studies beginning in 1985, researchers used a modeling scheme in which several thin two-dimensional regions were coupled together using a string model (Alipour-Haghighi & Titze, 1985; Berry et al., 1994; Alipour and Titze, 1996). This approach significantly reduced the computational

expense associated with full three-dimensional modeling, and allowed Alipour and his colleagues to study trajectories of vocal fold motion, modes of vibration, fluid–structure interactions, and acoustic coupling. However, this approach requires a large investment in the development of customized finite element modeling capabilities. Three-dimensional vocal fold models have also been utilized, but due to the computational expense associated with these models, many have focused on issues other than fluid–structure interactions. For example, de Vries et al. (1999) used static deformation and modal analysis simulations to create lumped mass models of vocal fold vibration. Gunter (2003) used static and dynamic simulations in the absence of fluid flow to examine vocal fold collisions. Hunter et al. (2004) used a three-dimensional model without fluid coupling to examine abduction and adduction of the vocal folds. The drawback of three-dimensional models is that they may require as much as two orders of magnitude more computational time and memory than two-dimensional models (Zheng, 2009).

Thomson et al. (2005) observed distinct differences between the vibratory characteristics of 2D and 3D models. The same phenomenon has since been mentioned by Cook and Mongeau (2007), Luo et al. (2008, 2009), Zheng (2009), and Zheng et al. (2009). Luo et al. (2008) addressed the problem by artificially modifying the mechanical properties of the 2D vocal fold model such that the modified model exhibited the same modal frequencies as a 3D model. This same approach was then followed in the subsequent studies cited above, all of which acknowledged the limitation of 2D models.

The purpose of this study is to confirm that differences between 2D and 3D vocal fold models are caused by the absence of shear stresses neglected by plane strain models (Cook and

\* Corresponding author. Tel.: +971 02 628 4192.

E-mail address: [douglascook@nyu.edu](mailto:douglascook@nyu.edu) (D. Cook).

Mongeau, 2007), and to develop an alternative approach for efficiently modeling the three-dimensional behavior and attributes of the vocal folds. These purposes are accomplished by introducing a new model that exhibits the vibratory characteristics of a three-dimensional model, but possesses the computational efficiency of a two-dimensional model. Furthermore, this model contains important physical information that is neglected by two-dimensional models, namely the vocal fold length and the influence of longitudinal shear modulus.

## 2. Methods

Consider a thin region of thickness  $w$ , one side of which lies at the center of an idealized vocal fold geometry (see Fig. 1). This region will be referred to as  $R$ . Previous formulations have modeled  $R$  as a region of plane strain because displacements, strains, and stresses vary only slightly across the thickness of  $R$ . However, when  $R$  is examined in the absence of the remaining vocal fold structure (as in a free body diagram), stresses are observed on the surfaces of  $R$ . The stresses acting on this region are  $\sigma_{yy}$ ,  $\sigma_{yx}$ , and  $\sigma_{yz}$ , ( $\sigma_{ij}$  represents the stress acting in the  $j$ -direction on the  $i$ -direction face). The plane strain modeling approach neglects all stresses acting on the  $y$  face of  $R$ . By including the stress components listed above, we can obtain an improved formulation that more accurately represents the three-dimensional characteristics of the vocal folds.

### 2.1. 2D/3D hybrid model formulation

The Ritz Method (Ritz, 1908) was used by Berry and Titze (1996) and Cook et al. (2007) in conjunction with an assumption of sinusoidal displacement to model the vocal folds. Based on the success of this approach, we also assume a vocal fold displacement field that is sinusoidal in the  $y$ -direction, while neglecting displacements in the anterior/posterior direction. The three-dimensional displacement field of the vocal folds is then expressed as notated in the following equations

$$U(x,y,z) = u_c(x,z)\sin\left(\frac{\pi y}{L}\right) \quad (1a)$$

$$V(x,y,z) = 0 \quad (1b)$$

$$W(x,y,z) = w_c(x,z)\sin\left(\frac{\pi y}{L}\right) \quad (1c)$$

In these equations,  $u_c$  and  $w_c$  represent the vocal fold displacements at the mid-coronal plane of the vocal folds.

To complete the model, we require the values of shear stresses that act on  $R$ . The normal stress component,  $\sigma_{yy}$ , acts perpendicular to  $R$ , and thus does not affect the motion of this region. Assuming a transversely isotropic material, Hooke's Law provides the following equations for the remaining stress components

$$\sigma_{yx} = G' \epsilon_{yx} \quad (2a)$$

$$\sigma_{yz} = G' \epsilon_{yz} \quad (2b)$$

Here,  $G'$  indicates the longitudinal shear modulus of the vocal folds and  $\epsilon_{ij}$  represents shear strain. The strain components depend upon displacements as

$$\epsilon_{yx} = \left(\frac{dU}{dy} + \frac{dV}{dx}\right) \quad (3a)$$

$$\epsilon_{yz} = \left(\frac{dW}{dy} + \frac{dV}{dz}\right) \quad (3b)$$

When the assumed forms of  $U$ ,  $V$ , and  $W$  are substituted in Eq. (3) and the resulting expressions substituted in Eq. (2), we obtain equations for the stresses acting on  $R$  as functions of the displacement of the plane strain model itself

$$\sigma_{yx} = \frac{G' \pi}{L} u_c(x,z) \cos\left(\frac{\pi y}{L}\right) \quad (4a)$$

$$\sigma_{yz} = \frac{G' \pi}{L} w_c(x,z) \cos\left(\frac{\pi y}{L}\right) \quad (4b)$$

Although the assumption of sinusoidal displacement does allow a derivation of the shear stresses acting on  $R$ , it consistently overestimates the magnitude of these stresses. This is because (a) the vocal fold displacement is not a true sinusoid (see Section 3.3), and (b) the shear stresses depend on the derivative of the assumed displacement pattern, which tends to exaggerate the discrepancy between our approximation and reality. Because the errors introduced by the sinusoidal assumption are consistent in nature, we have found that the application of a correction factor effectively offsets the problems mentioned above. The inclusion of a constant scalar correction factor ( $S$ ) results in the following modifications to Eqs. (4a) and (4b):

$$\sigma_{yx} = S \frac{G' \pi}{L} u_c(x,z) \cos\left(\frac{\pi y}{L}\right) \quad (5a)$$

$$\sigma_{yz} = S \frac{G' \pi}{L} w_c(x,z) \cos\left(\frac{\pi y}{L}\right) \quad (5b)$$

The final model (referred to hereafter as the “hybrid” model) consists of a regular plane strain computational domain with the shear stresses of Eqs. (5a) and (5b) added as displacement dependent loads. As opposed to the plane strain model, the hybrid model produces a full 3D deformation field (based on the Eqs. (1a)–(1c)). This feature is illustrated in Fig. 2, which depicts typical displacement patterns for plane strain and hybrid models.

The value of  $S$  in equation 5, is determined by minimizing the difference between results of a hybrid and a corresponding 3D model. As will be shown in the results section, a constant value for  $S$  produces results that are very similar to the 3D model, even as various model parameters are varied. It should be noted that the value of  $S$  depends on the type of analysis being performed (i.e. the value of  $S$  that is appropriate for static deformation may not be optimal for modal analysis).

### 2.2. Determining the accuracy of the 2D/3D Hybrid model

The validity of the hybrid model was thoroughly tested by comparing displacement magnitudes, displacement patterns, and modal frequencies of plane strain, hybrid, and 3D models.

All models possessed the same coronal geometry, shown in Fig. 3. The external geometry was based on the M5 geometry proposed by Scherer et al. (2001a). Table 1 gives the properties of the model. The 3D models were formed by extrusion of the 2D profile of Fig. 3A. All motion was restricted at the anterior, posterior, and lateral boundaries.

Static deformation simulations were used to assess each model's stiffness characteristics, given an applied pressure loading. The same pressure profile, consisting of a pressure function, which decreased linearly from an amplitude of  $P$  at point A, to zero at point B (Fig. 3A), was applied to all models to allow direct comparison. Modal analysis was used to assess dynamic characteristics of the models as it has been well established that the vibratory modes of the vocal folds are closely related to the fundamental frequency of vocal fold vibration (Titze, 1988; Berry et al., 1994; Svec et al., 2000; Zhang et al., 2007; Zhang, 2009; Luo et al., 2008, 2009; Zheng, 2009; Zheng et al., 2009).

One of the limitations of the plane strain approach is that it neglects key features of the actual vocal fold physiology such as vocal fold length and longitudinal shear modulus. Using a detailed three-dimensional model of the vocal folds, Cook et al. (2009) and Cook (2009) found that the latter features were

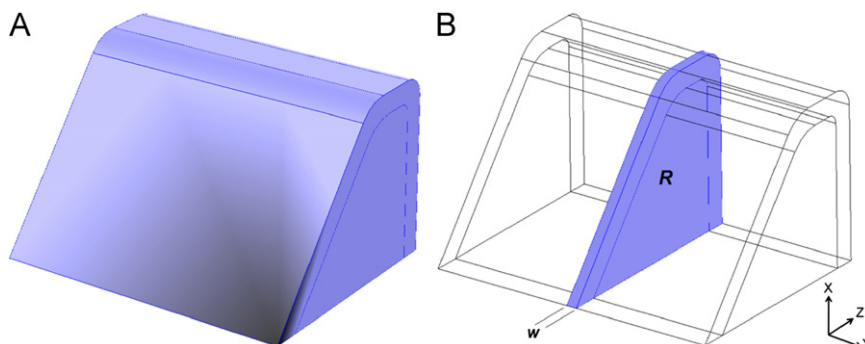
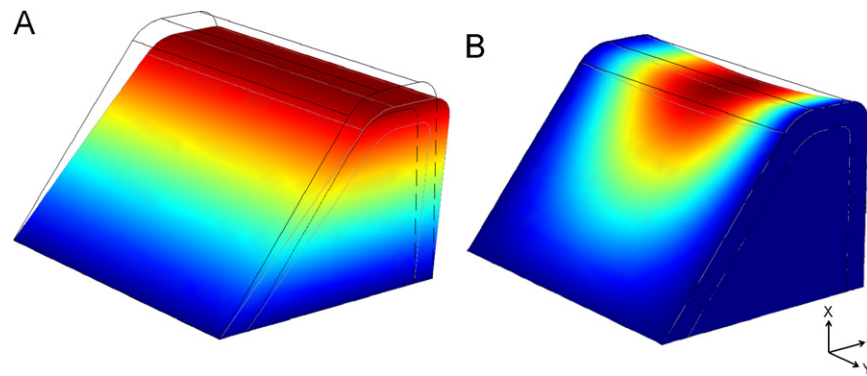
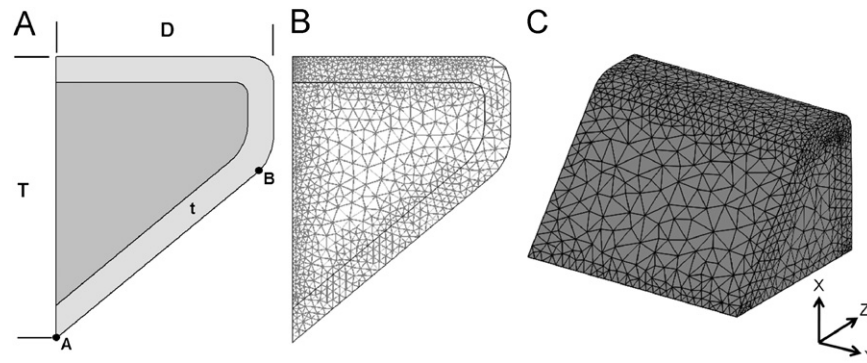


Fig. 1. Isometric (3D) view of an idealized (M5, Scherer et al., (2001b)) vocal fold geometry as seen from an inferior position.



**Fig. 2.** Illustration of typical three-dimensional displacement patterns for (A) plane strain, and (B) hybrid model. Because plane strain simulations cannot account for longitudinal variations, the plane strain solution is constant in the anterior/posterior direction. Color represents total displacement on the surface of each model. (This is a qualitative illustration and not a quantitative depiction of data.)



**Fig. 3.** Model geometry and computational meshes. (A) Coronal geometry profile used in the creation of all models, (B) computational domain for plane-strain and hybrid models (7.6 k dof), and (c) computational domain for three-dimensional models (115 k dof).

**Table 1**  
Geometric and material properties for the models used in this study.

Parameter	Symbol	Nominal Value	Applicable models:		
			Plane strain	Hybrid	3D
Length	$L$	14.3 mm		X	X
Depth	$D$	8.5 mm	X	X	X
Thickness	$T$	11 mm	X	X	X
Cover thickness	$t$	1 mm	X	X	X
Cover Stiffness	$E_c$	5 kPa	X	X	X
Transverse Young's Modulus	$E_b$	10 kPa	X	X	X
Longitudinal Young's Modulus	$E'$	30 kPa		X	X
Longitudinal Shear Modulus	$G'$	20 kPa		X	X

highly influential of vocal fold vibratory characteristics. To further assess the validity of the hybrid model, vocal fold length and longitudinal shear modulus were independently varied in all models (except the plane strain model, which has no dependence on these parameters).

### 2.3. Implementation details

The hybrid model was implemented using the commercial FEM code, COMSOL Multiphysics. The stresses in equations 4 (or 5) were applied as stress loads (force per unit area) in the respective directions on planar computational domain. The values  $u_c$  and  $w_c$  were based on the respective displacements of the computational domain.

## 3. Results

Because the three-dimensional model is based on fewer modeling assumptions than any other models, we assume that this

model is most accurate. Therefore all references to “accuracy” or “relative error” are with respect to the three-dimensional model.

Determination of the correction factor,  $S$  was performed for static and modal analysis using the nominal set of parameters given in Table 1. A single factor of 0.40 was used for all static analyses and a factor of 0.58 was used for all modal analyses presented below. Finally, for reference purposes, simulations were also performed for the case of no correction factor (Eqs. (4a) and (4b)).

### 3.1. Static deformation

The response of various models when subjected to static pressure loading is shown in Fig. 4. As seen in this figure, the plane strain model is much more compliant than the 3D model, but the hybrid model provides an excellent approximation of the 3D model. Because of reasons given in Section 2.1, the uncorrected hybrid model is less compliant than the 3D model.

In Fig. 4B–D, the applied pressure was held constant at 500 Pa while key parameters ( $E_c$ ,  $L$ , and  $G'$ ) were varied independently. In addition to the error magnitude, the plane strain model also behaves differently than the other models as model parameters are varied. For example, in Figs. 4C and D, the plane strain deformation is constant. This is because plane strain model results are independent of length and because the plane strain model does not utilize the parameter  $G'$ . On the other hand, both hybrid models approximate the trends of the three-dimensional model.

### 3.2. Modal analysis

All results in this section are restricted to the x-10 and x-11 modes of vibration, which have been shown to be responsible for

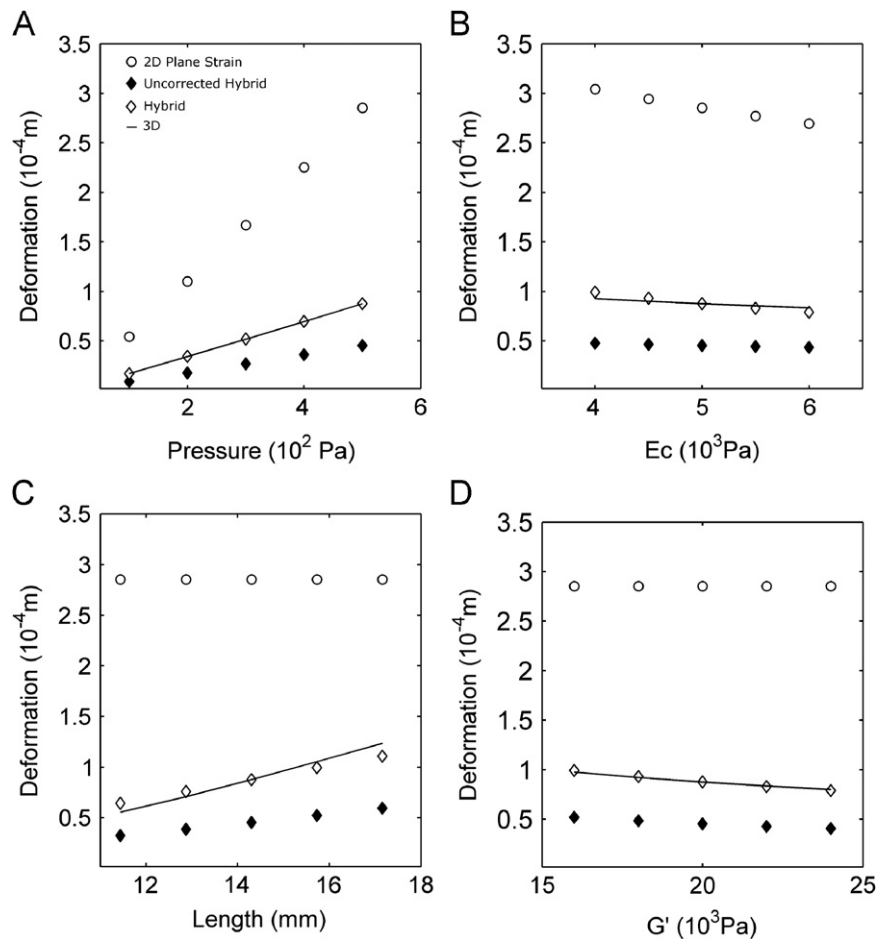


**Fig. 4.** Static deformation at the inferior point of a mid-coronal cross-section of the vocal folds. (A) static deformation as a function of pressure amplitude, (B) static deformation as a function of  $E_c$  ( $P=500$  Pa), and (C) static deformation as a function of  $L$  ( $P=500$  Pa); D) static deformation as a function of  $G'$  ( $P=500$  Pa).

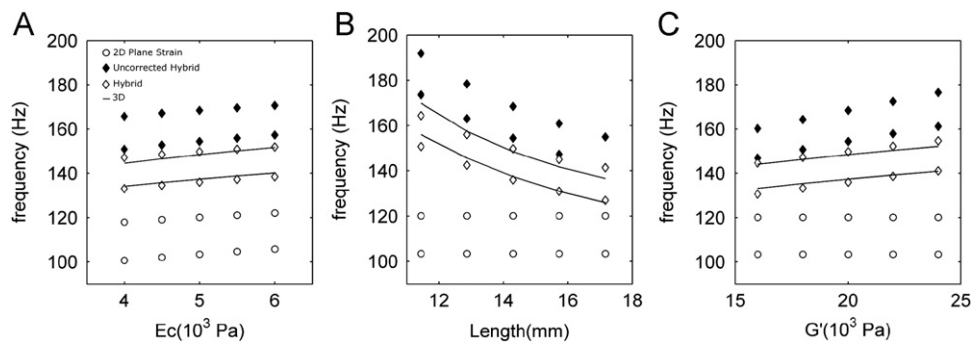


**Fig. 5.** Modal frequencies of x-10 and x-11 mode shapes for plane strain, hybrid, and three-dimensional models. For each model, the higher modal frequency represents the x-11 mode while the lower modal frequency represents the x-10 mode.

oscillation of the vocal folds (Titze and Strong, 1975; Berry et al., 1994). For variations in cover stiffness ( $E_c$ , Fig. 5A), all models exhibit similar behavior, with modal frequency rising in response to  $E_c$ . However, in Fig. 5B and C, the plane strain model results are constant whereas the 3D and hybrid models exhibit similar dependence on length and longitudinal shear modulus.

The modal frequencies of the plane strain model ranged from 16 to 53 Hz lower than those of the 3D model (12% to 34% relative error). The uncorrected hybrid model produced modal frequencies that were on average 18.5 Hz higher than the 3D model (13% error). The hybrid model provided the best approximation to the 3D modal frequencies with 93% of all modal frequencies falling

within 5 Hz of the 3D model values. The average absolute relative error of the hybrid model was less than 1%.

### 3.3. Hybrid model displacement patterns

Static deformation comparisons between models are shown in Fig. 6A, while mode shape comparisons are shown in 6B and C. In static deformation, the plane strain model exhibits a displacement that is significantly higher than the hybrid and three-dimensional models and is constant in the anterior/posterior direction. In the coronal plane (Fig. 6D), the plane strain model exhibits significant displacement in the superior (z) direction,

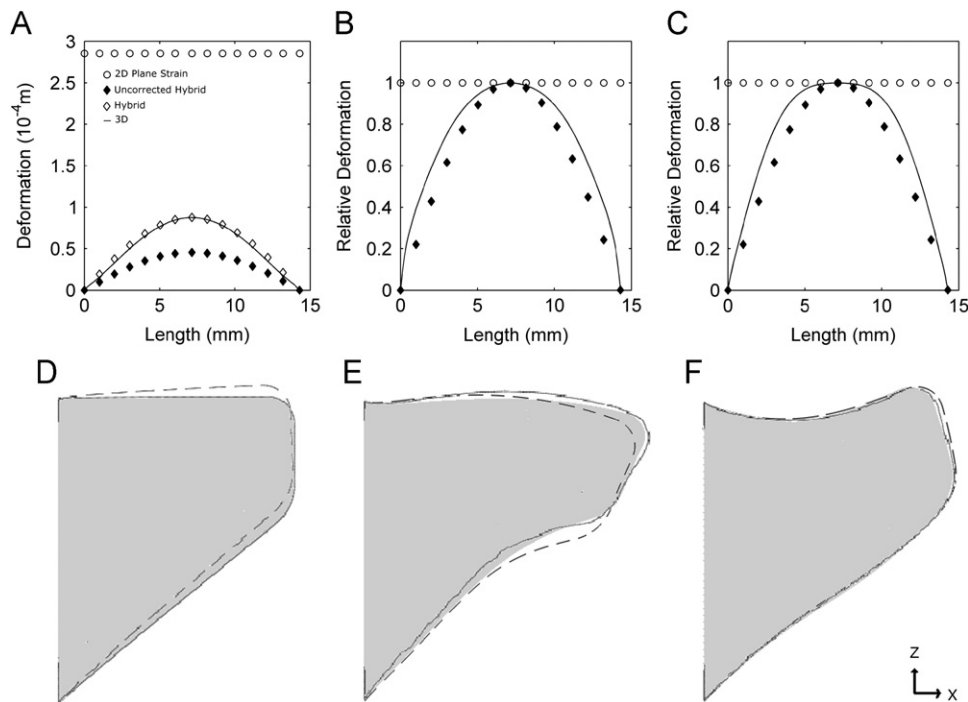


**Fig. 6.** Displacement pattern comparisons. (A) displacement as a function of anterior/posterior location along the medial surface of the vocal folds, and (B) displacement in the coronal plane: three-dimensional model (grey region); hybrid model (solid black); plane-strain (dotted). (constrained model omitted for clarity).

**Table 2**

Accuracy and computational expense comparisons between models and across analysis types. Error calculated relative to 3D model. Results followed by parentheses indicate averages, with standard deviations inside the parentheses.

		Model type			
Analysis type		Plane strain	Uncorrected hybrid	hybrid	3D
Relative error	Static	230% (54%)	–48%(2%)	0.5%(5.3%)	0%
	Modal	–22%(4.6%)	–13%(1.2%)	–0.1%(1.6%)	0%
Degree of freedom		7.6 k	7.6 k	7.6 k	57.6 k
CPU time (sec)	Static	1.01(0.19)	0.937(0.01)		75.4(11.3)
	Modal	0.655(0.01)	0.739(0.02)		21.8(1.17)

whereas the displacement of the hybrid model closely approximates the displacement pattern of the three-dimensional model.

Because mode shapes (eigenvectors) have no inherent magnitude, comparisons between mode shapes was accomplished by normalizing the curve of each model by its maximum value. Comparisons of mode shapes are given in Fig. 6B and C (anterior/posterior) and Fig. 6E and F (coronal). As observed in Fig. 6, the sinusoidal displacement assumption provides a reasonable approximation of the vocal fold displacement pattern even though some differences do exist.

### 3.4. Accuracy and computational expense comparisons

The relative errors of all data from Figs. 4 and 5 are summarized in Table 2. For both static and modal analysis, the hybrid model provided excellent accuracy, the uncorrected hybrid model provided moderate accuracy, and the plain strain model provided very poor accuracy. Not only is the hybrid model much more accurate than the plane strain model, but it requires about the same amount of computational expense. The processing times (CPU time) for various model and analysis types are also tabulated in Table 2. The lower computational cost of the hybrid

model(s) in static analysis is due to the fact that more iterations are required to resolve the large deformations of the plane strain model.

## 4. Discussion

### 4.1. Limitations of plane strain models

We have shown that the plane strain model is limited in several respects. All of the limitations of the plane strain model arise from the fact that it neglects important geometric and material properties of the vocal folds. First, the plane strain model is more compliant under static deformation than a three-dimensional model. Second, a plane strain model will always have modal frequencies that are lower than those of a corresponding three-dimensional model. Third, a plane strain model has no dependence on vocal fold length. Since length has long been known to be highly influential on vocal fold vibration (Friederich et al., 1993; Perkins and Kent, 1986), this may be the greatest weakness of the plane strain approach. Fourth, the plane strain model has no dependence on  $G'$ , which has been observed to be



highly influential for vocal fold vibratory characteristics (Cook et al., 2009). These issues account for the discrepancies between 2D and 3D models mentioned in previous studies.

Although the plane strain model is cheaper computationally, the limitations of this approach impose serious limitations on the value of the plane strain model as a research tool.

#### 4.2. Advantages of the 2D/3D hybrid model

The hybrid model compensates for many of the weaknesses of the plane strain model. The specific advantages of the hybrid model are as follows. First, the hybrid model accurately predicts the behavior of a three-dimensional model. Second, the hybrid model has an explicit length parameter, which results in length trends that are similar to those observed in a three-dimensional model. Third, the hybrid model includes the effects of the longitudinal shear modulus. Fourth, the hybrid model allows calculation of a full three-dimensional deformation field, an effect that is not possible with plane strain models. Finally, the computational expense of the hybrid model is comparable to that of the plane strain model and many times faster than a 3D model.

#### 4.3. Limitations of the hybrid model

Every model has its advantages and disadvantages. The hybrid model is based on an assumption of sinusoidal displacement in the y-direction, and no displacement in the anterior/posterior direction (see Eq. (1)). The hybrid model is thus unable to account for other displacement patterns. The creation of a hybrid model requires one simulation of a corresponding 3D model in order to obtain an appropriate correction factor. However, we have observed that a correction factor of 0.5 provides reliable results (error less than 15%) for both static and modal analyses.

The hybrid model is thus best suited for situations of regular phonation where anterior/posterior irregularities are not present, and where the vocal folds can be expected to exhibit vibration that is symmetric about the mid-coronal plane. The motion need not be sinusoidal in time (i.e. transient and chaotic effects can be captured), but the displacement pattern must be sinusoidal in the y-direction.

## 5. Conclusion

The inclusion of shear stresses (which are neglected in plane strain models) has been shown to account for the discrepancies previously observed between 2D and 3D vocal fold models. The inclusion of these stresses and an assumption of anterior/posterior displacement can be used to correct for these effects. The hybrid vocal fold model exhibits static and dynamic characteristics that are very similar to those of a full three-dimensional model. These similarities persist as length, cover stiffness, and longitudinal shear modulus are varied. In comparison to a plane strain model of the vocal folds, the hybrid model was in all cases much more accurate. Although more accurate than a plane strain model, the hybrid model requires the same computational expense. Finally, the hybrid model produces a three-dimensional displacement field similar to that of a three-dimensional model. The hybrid model therefore appears to be an excellent alternative to plane strain models since it captures important three-dimensional effects of the vocal folds without the added computational expense of a three-dimensional model.

## Conflict of Interest Statement

None of the authors have any conflict of interest to report.

## References

- Alipour-Haghighi F., and Titze I.R., 1985, Simulation of particle trajectories of vocal fold tissue during phonation, *Vocal Fold Physiology: Biomechanics, Acoustics, and Phonatory Control*. Ed. by Titze and Scherer, Denver Center for the Performing Arts, Denver, CO, USA.
- Alipour, H., Titze, I.R., 1996. Combined simulation of airflow and vocal fold vibrations, vocal fold physiology, controlling complexity and chaos. In: Davis, P., Fletcher, N. (Eds.), *Singular Publishing Group*, San Diego, pp. 17–29.
- Berry, D.A., Titze, I.R., 1996. Normal modes in a continuum model of vocal fold tissues. *Journal of the Acoustical Society of America* 100, 3345–3354.
- Berry, D.A., Herzel, H., Titze, I.R., Krischer, K., 1994. Interpretation of biomechanical simulations of normal and chaotic vocal fold oscillation with empirical eigenfunctions. *Journal of the Acoustical Society of America* 95, 3595–3604.
- Cook, D.D., Mongeau, L., 2007. Sensitivity of a continuum vocal fold model to geometric parameters, constraints, and boundary conditions. *Journal of the Acoustical Society of America* 121, 2247–2253.
- Cook, D.D., Nauman, E., Mongeau, L., 2009. Ranking vocal fold model parameters by their influence on modal frequencies. *Journal of the Acoustical Society of America* 126 (4), 2002–2010.
- Cook, D.D., 2009. Systematic structural analysis of human vocal fold models, Ph.D. Dissertation, Purdue University, USA.
- Decker, G.Z., Thomson, S.L., 2007. Computational simulations of vocal fold vibration: Bernoulli versus Navier-Stokes. *Journal of Voice* 21 (3), 273–284.
- de Vries, M.P., Schutte, H.K., Verkerke, G.J., 1999. Determination of parameters for lumped parameter models of the vocal folds using a finite-element method approach. *Journal of the Acoustical Society of America* 106, 3620–3628.
- Friederich, G., Kainz, J., Freidl, W., 1993. Zur funktionellen struktur der menschlichen stimm lippe. *Laryngo-Rhino-Otol* 72, 215–224.
- Gunter, H., 2003. A mechanical model of vocal-fold collision with high spatial and temporal resolution. *Journal of the Acoustical Society of America* 113, 994–1000.
- Hunter, E.J., Titze, I.R., Alipour, F., 2004. A three-dimensional model of vocal fold abduction/adduction. *Journal of the Acoustical Society of America* 115, 1747–1759.
- Liljencrants, J., 1985, Speech synthesis with a reflection-type line analog, Ph.D. Dissertation, Royal Institute of Technology, Stockholm, Sweden.
- Luo, H., Mittal, R., Zheng, X., Bielamowicz, S.A., Walsh, R.J., Hahn, J.K., 2008. An immersed-boundary method for flow-structure interaction in biological systems with application to phonation. *Journal of Computational Physics*, 9303–9332.
- Luo, H., Mittal, R., Bielamowicz, S.A., 2009. Analysis of flow-structure interaction in the larynx during phonation using an immersed-boundary method. *Journal of the Acoustical Society of America* 126 (2), 816–824.
- Perkins, W., Kent, R., 1986. *Functional Anatomy of Speech, Language, and Hearing: A Primer*. Allyn and Bacon, Boston, MA.
- Ritz, W., 1908. U ber eine neue Methode zuer Lösung gewisser Variations problemeder mathematischen Physik. *Journal für die reine und angewandte Mathematik* 135, 1–61.
- Scherer, R.C., De Witt, K.J., Kucinski, B.R., 2001a. The effect of exit radii on intraglottal pressure distributions in the convergent glottis. *Journal of the Acoustical Society of America* 110 (5), 2267–2270.
- Scherer, R.C., Shinwari, D., De Witt, K.J., Zhang, C., Kucinski, B.R., Afjeh, A.A., 2001b. Intraglottal pressure profiles for a symmetric and oblique glottis with a divergence angle of 10 degrees. *Journal of the Acoustical Society of America* 109 (4), 1616–1630.
- Story, B.H., 1995. Physiologically-based speech simulation using an enhanced wave-reflection model of the vocal tract, Ph.D. dissertation, University of Iowa.
- Svec, J.G., Horáček, J., Sram, F., Vesely, J., 2000. Resonance properties of the vocal folds: In vivo laryngoscopic investigation of the externally excited laryngeal vibrations. *Journal of the Acoustical Society of America* 108, 1397–1407.
- Thomson, S.L., Mongeau, L., Frankel, S.H., 2005. Aerodynamic transfer of energy to the vocal folds. *Journal of the Acoustical Society of America* 118 (3), 1689–1700.
- Titze, I.R., Strong, W.J., 1975. Normal modes in vocal cord tissues. *Journal of the Acoustical Society of America* 57, 736–744.
- Titze, I.R., 1988. The physics of small-amplitude oscillation of the vocal folds. *Journal of the Acoustical Society of America* 83, 1536–1552.
- Zhang, Z., Neubauer, J., Berry, D.A., 2007. Physical mechanisms of phonation onset: a linear stability analysis of an aeroelastic continuum model of phonation. *Journal of the Acoustical Society of America* 122 (4), 2279–2295.
- Zhang, Z., 2009. Characteristics of phonation onset in a two-layer vocal fold model. *Journal of the Acoustical Society of America* 125 (2), 1091–1102.
- Zheng X., 2009. Biomechanical Modeling Of Glottal Aerodynamics And Vocal Fold Vibration During Phonation, Ph.D. Dissertation, The George Washington University, Washington D.C., USA.
- Zheng, X., Bielamowicz, S., Luo, H., Mittal, R., 2009. A computational study of the effect of false vocal folds on glottal flow and vocal fold vibration during phonation. *Annals of Biomedical Engineering* 37 (3), 625–642.